Top Catal (2008) 49:18–23
DOI 10.1007/s11244-008-9067-2

ORIGINAL PAPER

The Influence of the Dipolar Field Effect on the Photochemical Reactivity of $Sr_2Nb_2O_7$ and $BaTiO_3$ Microcrystals

Jennifer L. Giocondi · Gregory S. Rohrer

Published online: 9 May 2008

Abstract It has previously been shown that the dipolar field effect spatially localizes photochemical reaction products on the surfaces of macroscopic ferroelectric crystals. In this work, photochemical reactions that deposit insoluble products on the surface have been used to study the dipolar field effect in microcrystals of $BaTiO_3$ and $Sr_2Nb_2O_7$. In both cases, the patterns of reduced silver on the surface were consistent with the orientations of the ferroelectric domains within the samples. The results show that dipolar fields associated with the ferroelectric domains in small particles can separate photogenerated charge carriers and spatially localize reaction products.

Keywords Dipolar field effect · Photochemical reactivity · $Sr_2Nb_2O_7$ · $BaTiO_3$

1 Introduction

Internal polarizations within ferroelectric solids create dipolar electric fields. These fields influence the transport of photogenerated charge carriers; this phenomenon is referred to as the bulk photovoltaic effect [1–6]. Because photogenerated carriers move in opposite directions in the static field, an open circuit voltage is observed that depends on the poling direction and the magnitude of the remanent polarization. The bulk photovoltaic effect also generates a photocurrent that is directly proportional to the light intensity and disappears above the Curie temperature, when the crystal loses its polarization [4]. The possibility that polarizations within ferroelectrics affect the kinetics of charge transfer at the catalyst surface led van Damme and Hall [7] to compare photocatalytic and ferrocatalytic effects in the oxidation of H_2 and CO.

A bulk ferroelectric is made up of individual domains that can be polarized in multiple directions. In the unpoled case, there are equal volumes of opposing domains so that the net polarization is zero. In poled materials, one type of domain makes up a greater fraction of the sample's volume than the others and the material has a net polarization. Inoue and co-workers [8, 9] studied the effect of poled ferroelectrics on water photolysis. Photoloysis experiments on poled $Pb(Zr_xTi_{1-x})O_3$ showed that 10–40 times more hydrogen was evolved from the positive polar surface than from the negative surface. This result suggests that the polarization direction affects the motion of photogenerated carriers so that the reduction half reaction is promoted by the positively poled surface while the oxidation half reaction is promoted by the negatively poled surface. The spatial separation of the two half reactions can potentially have a beneficial effect on the photolysis efficiency. After charge is transferred from the catalyst to adsorbed species on the surface, the reduced and oxidized intermediates can recombine rather than generate molecular hydrogen or oxygen. The back reaction reduces the efficiency of the process and is more likely to occur if the sites of reduction and oxidation are in close proximity. If reduction and oxidation occur on different surfaces, then the back reaction is suppressed. However, later experiments on poled and unpoled $Pb_{1-x}K_{2x}Nb_2O_6$ did not reproduce the same effect [10].

J. L. Giocondi · G. S. Rohrer (✉)
Department of Materials Science and Engineering, Carnegie Mellon University, Pittsburgh, PA 15213-3890, USA
e-mail: gr20@andrew.cmu.edu

Present Address:
J. L. Giocondi
Lawrence Livermore National Laboratory, Chemistry and Materials Science Directorate, P.O. Box 808, L-367, Livermore, CA 94551-9900, USA

Recent results from experiments on unpoled samples have demonstrated that the spatial separation of reaction products can also occur on the scale of individual domains [11, 12]. In these experiments, photochemical reactions that leave insoluble reaction products on the surface are used to examine both the reduction and oxidation half reactions. Silver cations from an aqueous solution are reduced on the surface of ferroelectric domains in $BaTiO_3$ when the polarization vector (positive polarization) is oriented toward the surface. Lead cations are oxidized on the domains with the opposite polarization. Therefore, a single surface is covered with patches that promote either reduction or oxidation. When the patches are sufficiently large, they may still localize reaction products in a way that suppresses the back reaction, without requiring charge to be separated over macroscopic distances. It is interesting to note that a similar domain specific reactivity has been observed at the surfaces of non-ferroelectric $SrTiO_3$ [13]. In this case, the localization of the reaction was attributed to polar surface terminations. Because polarization from ferroelectric domains and polar surface terminations cause a similar localization of reduction and oxidation products, we refer to this phenomenon as the dipolar field effect.

Previously, the dipolar field effect has been observed only in bulk materials. The objective of the present paper is to report the dipolar field effect in microcrystals. Experiments are conducted on faceted crystals of two different ferroelectric materials: $BaTiO_3$ and $Sr_2Nb_2O_7$. From observations of the locations at which reaction products form on the surface, it is clear that the dipolar field effect influences the motion of photogenerated carriers in these crystals and that in the case of single domain crystals, the reduction and oxidation half reactions can be separated to opposite sides of the same single crystal.

2 Experimental

$Sr_2Nb_2O_7$ powders were obtained by reacting stoichiometric ratios of $SrCO_3$ (Alfa Aesar 99%, pure) and Nb_2O_5 (Alfa Aesar, 99.5% pure) in air at 1,400 °C for 100 h. Powder X-ray diffraction was used to confirm the phase purity. $BaTiO_3$ powders were obtained from a commercial source (Alfa Aesar, 99.7% pure). Small, faceted $BaTiO_3$ and $Sr_2Nb_2O_7$ crystals were produced using a molten salt flux method. Equal weights of the target phase and KCl (Fisher Scientific) were combined by wet grinding in ethanol for several minutes. The slurry was then transferred to a Pyrex beaker and mixed by magnetic stirring for 2 h. Following mixing, the excess ethanol was decanted with a pipet and the powders were dried in air at 70 °C. The dried powder was transferred to an Al_2O_3 crucible and heated in air at 5 °C/min to 1,100 °C for 6 h. The KCl was removed by filtering with boiling deionized water and the remaining product was dried in air at 70 °C. The identity of the phase was confirmed by powder X-ray diffraction.

Two photochemical reactions were used to identify reactive facets: the reduction of Ag^+ by photogenerated electrons and the oxidation of Pb^{2+} by photogenerated holes. These reactions are:

$$Ag^+ + e^- = Ag, \quad (1)$$

$$Pb^{2+} + 2H_2O + 2h^+ = PbO_2 + 4H^+. \quad (2)$$

Both reactions leave an insoluble product on the surface (Ag and PbO_2, respectively) that can be observed in a scanning electron microscope. Reaction (1) is completed by the oxidation of hydroxyls and reaction (2) is completed when electrons reduce H^+. These reactions are not directly observed. The photochemical reaction experiments are setup in two different ways, with similar results. In the first, an SEM stub covered by carbon tape was dusted with the powder. After removing the excess powder with forced air, a viton O-ring, 1.7 mm thick, was placed on the sample surface and the interior volume was filled with a solution containing a dissolved metal salt. For the reduction reaction, 0.115 M aqueous $AgNO_3$ (Fisher Scientific) was used and for the oxidation reaction, 0.0115 M aqueous $Pb(C_2H_3O_2)_2$ (Fisher Scientific) was used. A 0.2 mm thick quartz cover slip was then placed on top of the O-ring and held in place by the surface tension of the solution. The sample was illuminated using a variable power Hg lamp (Oriel). Exposures of 10 s to 300 s at a lamp power of 300 W were used for the reduction of Ag^+ and the oxidation of Pb^{++} on the two materials. After exposure, the sample was rinsed with deionized H_2O and dried with forced air. The second method was to irradiate a suspension of particles in a continuously stirred, 0.0115 M aqueous $AgNO_3$ solution contained in a Pyrex reaction vessel. A water-cooled quartz inner irradiation cell (450 W high-pressure Hg lamp) was suspended into the bath. The reactor was evacuated and filled with Argon three times and then Ar was bubbled through the suspension for the remainder of the experiment. The particles were illuminated for 45 min, filtered, rinsed with deionized water, and dried. A number of control experiments described in detail elsewhere confirm that deposits are formed only when the light source contains photons with an energy greater than the band gap, reaction products are not formed homogeneously in solution during illumination, and that chemically generated colloidal silver does not attach to the surface [14]. In other words, we are certain that the observed reaction deposits are produced by a photochemical reaction on the crystal surface.

Scanning electron microscopy (SEM, Phillips XL30FEG) was used to examine the surfaces of as-processed and

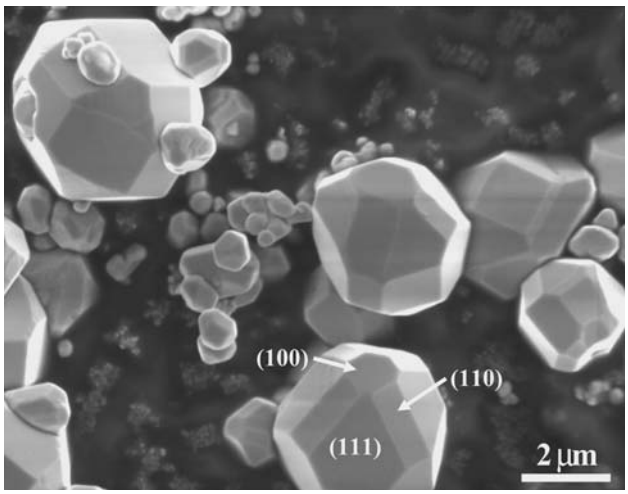

Fig. 1 SEM images of faceted $BaTiO_3$ crystals produced in a KCl flux. The crystallographic orientations of the faces are labeled

as-reacted particles. Typical imaging conditions were: working distance = 10 mm, spot size = 3 or 4, and accelerating voltage = 5–10 kV. For the $BaTiO_3$ crystals, the orientation assignments for the facets planes were made by symmetry. The orientations of the $Sr_2Nb_2O_7$ were determined using electron backscattered patterns. Patterns were collected using a Phillips XL40FEG SEM and indexed using Orientation Imaging Microscopy Software, Windows Software version 3 (TexSEM Laboratories, Inc.). Energy dispersive X-ray (EDX) spectroscopy (Oxford Isis) conducted in a scanning electron microscope (Phillips XL30FEG) was used to analyze the elemental composition of the deposits. It was confirmed that the deposits from the silver reduction reaction contained Ag and that deposits from the lead oxidation reaction contained Pb.

3 Results

The SEM image in Fig. 1 shows the as-prepared $BaTiO_3$ crystals. Most crystals are bounded by {100}, {110}, and {111} type planes, as indicated in the figure, and have diameters in the range of 1–5 μm. The shapes of these crystals were determined above the Curie temperature, when their symmetry was cubic. Therefore, facet orientations were assigned based on the symmetry and multiplicity of each plane. Polarizations in each domain are aligned in one of the cubic <100> directions. No domain boundaries are observed on the surfaces of the as-prepared crystals.

When the crystals are illuminated in the presence of aqueous $AgNO_3$, some of the domains become covered by silver (see Fig. 2). The SEM images clearly show striped patterns of silver on the surfaces of multi-domain crystals that are similar to what is observed on macroscopic single crystals [11, 12]. While the spatial distribution of reduced silver is primarily determined by the domain structure, there is also an apparent dependence on the surface orientation. After inspecting many micrographs such as those shown in Fig. 2, the relative reactivity of the faces can be ranked as {100}>{111}>{110}.

In some crystals, only a single domain was apparent. In these cases, silver was deposited on only one of the exposed {100}-type faces (see Fig. 3). The reactivity on this face is much higher than on any of the other faces. Interestingly, the highly reactive face was surrounded by an unreactive region, a fraction of a micron in width, near the edge of the face. The abruptness of the boundaries between the reactive and unreactive areas suggests that domains of opposite polarization were formed near the edges of the reactive face to minimize the total electrostatic energy.

$BaTiO_3$ crystals after reaction in the lead acetate solution are shown in Fig. 4. Evidence for lead oxidation is found on the {100}, {110}, and {111} surfaces. However, as was for the case of the silver reduction reaction, the coverage is not uniform. For example, there are uncovered areas on the (100) and (110) facets of the crystal in Fig. 4a and only about half of the (111) face of the crystal in 4b is covered with lead containing deposits.

The SEM images in Fig. 5 show the appearance of the as prepared $Sr_2Nb_2O_7$ crystals. The majority of the crystals

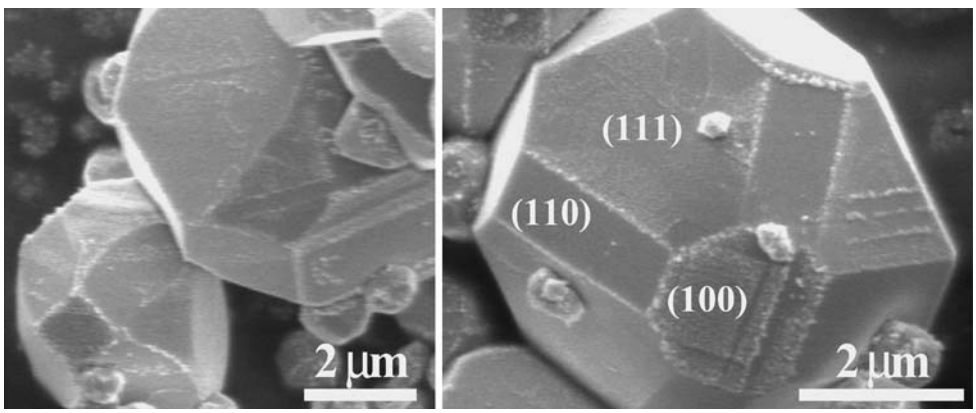

Fig. 2 SEM images of faceted $BaTiO_3$ crystals after reaction in aqueous $AgNO_3$. The speckled white contrast corresponds to silver containing deposits. The striped pattern of these deposits is consistent with the domain structure and polarization specific reactivity

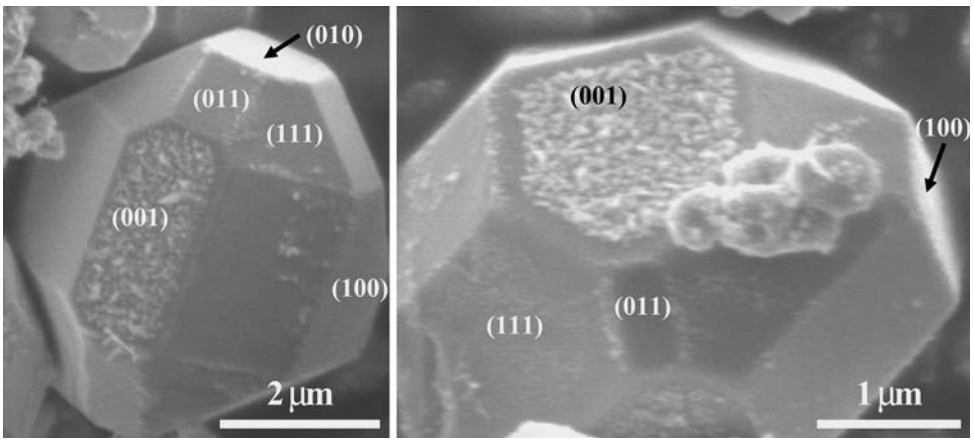

Fig. 3 SEM images of faceted $BaTiO_3$ crystals after reaction in aqeous $AgNO_3$. The speckled white contrast corresponds to silver containing deposits. The patterns of silver indicate that the crystals have a single domain

were found in agglomerates containing large, thin rectangular platelets with high aspect ratios. Based on electron backscattered diffraction patterns, the largest face has the (010) orientation and the crystals are elongated in the [100] direction. The long and short edges of the crystal are most likely bounded by {001} and {100} type planes respectively. The platy habit mimics the internal structure of the compound, which is comprised of (110)-orientated perovskite-like slabs separated by SrO layers stacked along the [010] axis [15]. $Sr_2Nb_2O_7$ is also a ferroelectric and, in this case, the polarization in each domain is oriented along one of the two <001> axes [16]. These directions are in the plane of the plate, perpendicular to the long axis of the plate.

No oxidized lead was observed on surfaces of the crystals following illumination in lead acetate solution. However, silver containing deposits were found with anisotropic distributions after illumination in silver nitrate solution. The majority of silver deposits are located at the step edges along the long axis of the large crystals, which is the [100] direction. The SEM images in Fig. 6 clearly show that the silver deposits on steps perpendicular to the <001> directions (this is the polarization axis of the crystal). The images also show that not all of the apparently identical

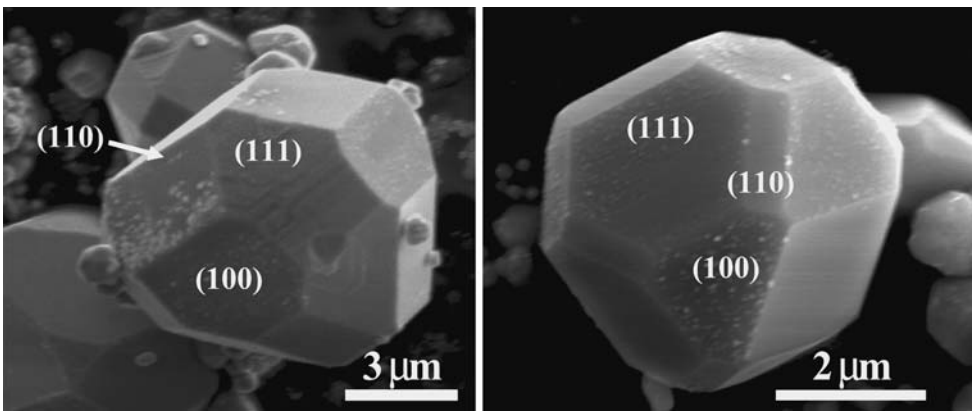

Fig. 4 SEM images of faceted $BaTiO_3$ crystals after reaction with aqueous $Pb(C_2H_3O_2)_2$. The white contrast corresponds to oxidized lead containing deposits. The pattern of these deposits is consistent with polarization specific reactivity on multidomain particles

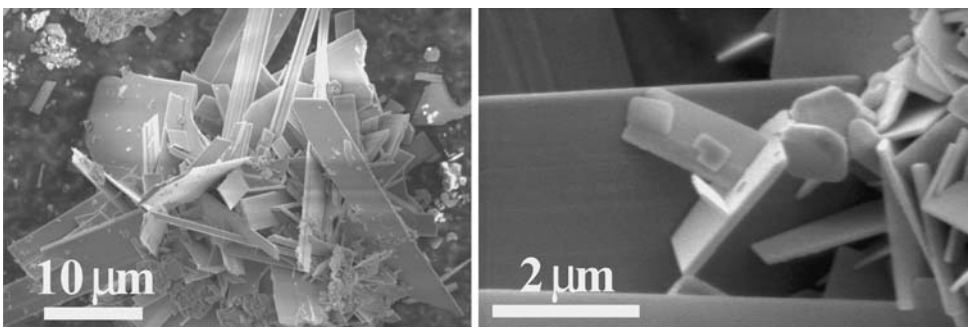

Fig. 5 Faceted $Sr_2Nb_2O_7$ crystals prepared in a KCl flux. The large faces of these particles are bounded by {010} type planes

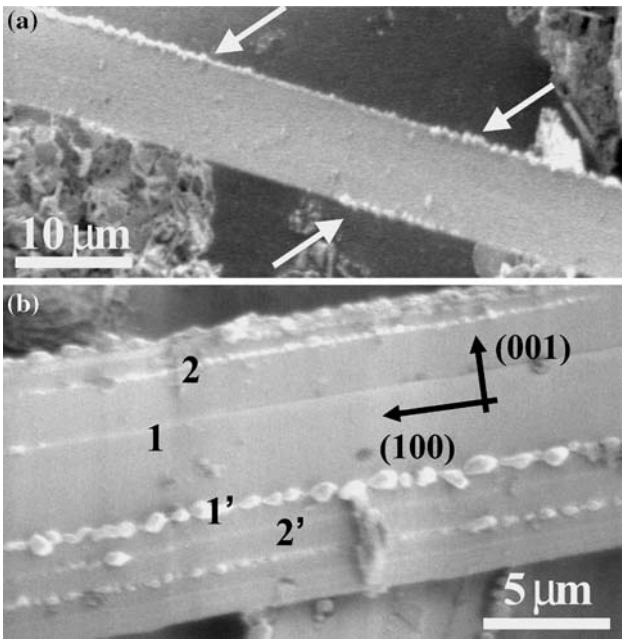

Fig. 6 SEM images of faceted $Sr_2Nb_2O_7$ crystals following the silver reduction reaction. (**a**) Arrows shows silver deposits alternating along the opposing long edges of the crystal. (**b**) Numbers indicate opposing terraces with different reactivity. The differential reactivity on opposing {001} edges indicates a polarization specific reactivity

steps are reactive and that the reactivity is not constant along the length of a single step. Fig. 6a shows a particle with reactivity only along the long edges of the particle. The arrows in this image indicate how the silver deposits alternate between opposing edges. In other words, when the upper edge is reactive, the lower edge is not, and vise versa. As mentioned earlier, these edges are most likely to be bounded by (001) planes, which are perpendicular to the direction of spontaneous polarization. The distribution of reaction products on the crystal shown in Fig. 6b has the same characteristics as the one in Fig. 6a. When silver is found on the edge of one terrace, it is absent from the opposite edge.

4 Discussion

The SEM images of the $BaTiO_3$ crystals after the photochemical reactions show spatially resolved reactivity that is similar to what is observed on bulk samples. The boundaries between the reactive areas and the unreactive areas are in most cases straight, which indicates the intersection of a 90° domain wall with the surface, and in other cases the boundaries are curved, which is characteristic of a 180° domain wall. The vast majority of the crystals observed had multiple domains. However, a few crystals, such as those Fig. 4, displayed a single domain that covered an entire {100}-type face. In such a crystal, the reduction reaction occurs on the (001) face and the oxidation reaction occurs on the $(00\bar{1})$ face.

$Sr_2Nb_2O_7$ is known to have a high efficiency for water photolysis [17, 18]. One possible explanation for this reactivity is that its complex layered structure creates chemically distinct surfaces that favor either reduction or oxidation. If the two half reactions are promoted by distinct bounding surfaces, then the spatial separation would have the effect of decreasing the rate at which the reduced and oxidized products back react to reform water, and this may lead to an increased efficiency. A second possible explanation is that the dipolar fields within the ferroelectric domain structure of $Sr_2Nb_2O_7$ act to separate both the photogenerated charge carriers and the reduced and oxidized products, again leading to more efficient photolysis.

Based on the current observations, the second of these two explanations seems more likely. Because apparently identical surfaces (the step edges along the [100] direction) do not have a uniform reactivity, the surface orientation is not the only factor influencing the reactivity. On the other hand, it is known that domains in $Sr_2Nb_2O_7$ are polarized along the [001] axis [16]. Within a domain, electrons will tend to move along the positive direction of the polarization vector, which might point in either the [001] or the $[00\bar{1}]$ direction, depending on the domain orientation. Therefore, if a single domain traverses the width of a crystal (along the [001] direction) and if by analogy with $BaTiO_3$, silver is reduced on the (001) surface of the crystal, it should not be reduced on the parallel $(00\bar{1})$ surface. This is exactly what is observed in Fig. 6. The numbers in Fig. 6b indicate opposite steps bounding the same terrace. For example, 1 and 1′ indicate an unreactive and reactive step, respectively. The reactivity of this terrace can be explained if the direction of the spontaneous polarization points from 1 to 1′ and electrons move in this direction. Similarly, if the spontaneous polarization points from the unreactive 2′ edge to the reactive 2 edge, the reactivity of this terrace can be explained. Therefore, a 180° domain wall lies within the (010) plane between terrace 1 and 2.

While the experiments reported here indicate that it is the (001) surfaces that are active for reduction, it should also be noted that $Sr_2Nb_2O_7$ only splits water with a high efficiency when it is promoted with Ni, and this was not used in the current experiments [17, 18]. While the promoter clearly influences the catalyst's reactivity, it will not alter the influence that the internal dipolar field has on the movement of the electrons and holes.

The fact that the dipolar field effect influences the reactivity of microcrystals implies that it might be an important property that determines the performance of photolysis catalysts. Figure 7 is a schematic illustration

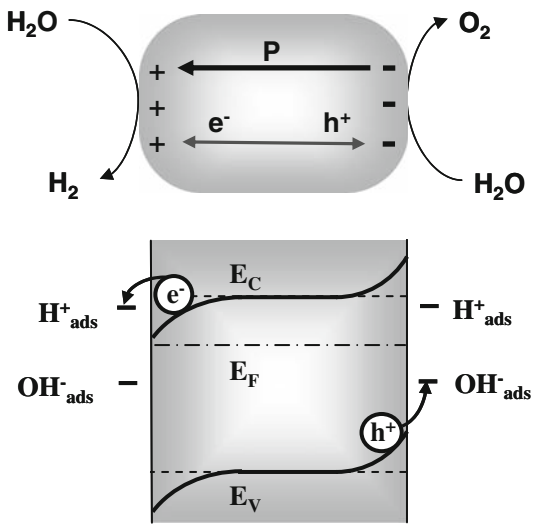

Fig. 7 Schematic illustration of how the bulk photovoltaic effect influences carriers in a small ferroelectric crystal. The polarization, P, forces the photogenerated electrons and holes to opposite sides of the particle and causes band-bending at the particle surface. This results in reduction and oxidation reactions, in the example here of water photolysis, that occur on different sides of the particle

depicting the process by which the dipolar field effect can influence the reactivity of individual ferroelectric catalyst particles. The internal polarization (P) will force electrons and holes towards opposite surfaces. The polarization should also lead to band bending at the surface that promotes the transfer of charge to absorbed species. The separation of photogenerated charge carriers reduces the probability that electrons and holes recombine before reacting with adsorbates. The localization of reaction products on opposite surfaces of the crystal reduces the probability that the reduced and oxidized intermediates (hydroxyl radicals and atomic hydrogen) back react to form water before forming more stable molecular species. We can speculate that the effect that this will have on the efficiency will be size dependent. If the particle is too small, then the spatial separation might not be large enough to suppress the back reaction. On the other hand, it the particle is too large, it is less likely that the electrons and holes are able to both reach a free surface.

5 Conclusions

The dipolar field effect, known to influence photochemical reactions in bulk samples, also causes the spatial localization of reaction products on the surfaces of ferroelectric microcrystals. Patterns of reduced silver on microcrystals of $BaTiO_3$ and $Sr_2Nb_2O_7$ were consistent with the orientations of the ferroelectric domains within the samples, indicating that the associated dipolar fields separated photogenerated charge carriers and spatially localize reaction products.

Acknowledgement This work was supported by the National Science Foundation under grant DMR-0412886.

References

1. Brody PS (1973) Solid State Commun 12:673
2. Glass AM, von der Linde D, Negran TJ (1974) Appl Phys Lett 25:233
3. Brody PS, Crowne F (1975) J Elect Mater 4:955
4. Brody PS (1975) J Solid State Chem 12:193
5. von Baltz R (1978) Phys Stat Sol B 89:419
6. Fridkin VM (1984) Ferroelectrics 53:169
7. van Damme H, Hall WK (1981) J Catal 69:371
8. Inoue Y, Sato K, Sato K., Miyama H (1986) J Phys Chem 90:2809
9. Inoue Y, Hayashi O, Sato K, Kubokawa T (1988) In: Proceedings of the 9th international congress on catalysis, Chemical Institute of Canada, Ottawa, p 1497
10. Inoue Y, Hayashi O, Sato K (1990) J Chem Soc Faraday Trans 86:2277
11. Giocondi JL, Rohrer GS (2001) J Phys Chem B 105:8275
12. Giocondi JL, Rohrer GS (2001) Chem Mater 13:241
13. Giocondi JL, Rohrer GS (2003) J Amer Ceram Soc 86:1182
14. Giocondi JL (2003) Ph.D. Thesis, Carnegie Mellon University
15. Ishizawa N, Murumo F, Kawamura T, Kimura M (1975) Acta Crystallogr B31:1912
16. Takahashi M, Namamatsu S, Kimura M (1972) J Cryst Growth 13/14:681
17. Hwang DW, Kim HG, Kim J, Cha KY, Kim YG, Lee JS (2000) J Catal 193:40
18. Kudo A, Kato H, Nakagawa S (2000) J Phys Chem B 104:571